Assessment of Transmission Factors and Shielding Requirements for Lead, Concrete, and Iron in PET Imaging Environments

KEM. Mohamadain, Zeinab K. Osman, N. Abbas Ahmad

1 Department of Physics, College of Science, Sudan University of Science and Technology, Khartoum, Sudan

2 Department of Physics, College of Science, Sudan University of Science and Technology, Khartoum, Sudan

3 Department of Physics, College of Science, Sudan University of Science and Technology, Khartoum, Sudan Zeinab K. Osman: zkhidero@yahoo.com

Abstract

Positron Emission Tomography (PET) facilities require tailored radiation shielding due to the highly penetrating 511 keV annihilation photons and the substantial construction costs associated with overly conservative designs. In many low-resource settings, the dependence on Monte Carlo–based calculations further limit the feasibility of establishing PET services. This study introduces a practical and cost-efficient shielding design approach based on analytical methods validated against published Monte Carlo–derived reference data. A certified architect developed a complete PET facility layout that meets international radiation safety and architectural standards. Using this plan, shielding requirements for lead, steel, and concrete were calculated through standard attenuation equations and compared with transmission data from the American Association of Physicists in Medicine (AAPM). The analytical method yielded shielding thicknesses of 0.089–0.81cm for lead, 0.20–1.87 cm for steel, and 0.98–8.91 cm for concrete—values that complied with safety limits while consistently remaining lower than Monte Carlo–based recommendations. These findings demonstrate that analytically derived designs, when applied to a realistic architectural layout, can achieve regulatory compliance without unnecessary over-shielding. The proposed approach offers a reliable, accessible, and economically advantageous alternative for institutions, particularly in low-resource regions, aiming to implement PET services safely and sustainably.

Keywords: PET shielding, radiation protection, facility design, analytical attenuation, Monte Carlo validation, cost optimization

Introduction:

Positron Emission Tomography (PET) is now a central tool in nuclear medicine, with established roles in oncology, neurology, and cardiology due to its high sensitivity and capacity for quantitative functional imaging [1–3]. Among available PET tracers, ^{18}F-fluorodeoxyglucose (^{18}F-FDG) remains the most widely used because of its practical half-life of 110 minutes and its suitability for centralized production and distribution [4]. Unlike conventional gamma emitters

such as ^{99m}Tc or ^{131}I, PET imaging relies on detection of two 511 keV annihilation photons, which are considerably more penetrating. As a result, PET facilities require more rigorous shielding design than standard nuclear medicine installations [5,6].

Radiation exposure to staff—especially during preparation and administration of radiopharmaceuticals—can be significant, with extremity and whole-body doses exceeding those typically encountered in routine nuclear medicine practice [7,8]. Therefore, facility layouts must comply with national regulations and international dose limits, including those set by the International Commission on Radiological Protection (ICRP) [13]. Guidance from the American Association of Physicists in Medicine (AAPM) Task Group 108 is widely used for PET shielding; however, its simplified source models and conservative assumptions often lead to overestimated barrier thicknesses, increasing construction costs unnecessarily [9–11]. More detailed modeling using Monte Carlo radiation-transport codes such as MCNP, FLUKA, and GATE/Geant4 has provided improved insight into scatter and buildup effects in realistic clinical environments [12–15]. Despite their accuracy, Monte Carlo methods require substantial computational resources and expertise, which may not be readily available in many institutions. In the present study, Monte Carlo simulations were not performed. Instead, analytical calculations based on exponential attenuation formulas and NIST XCOM data were compared directly with previously published Monte Carlo–derived transmission tables from AAPM. A certified architect prepared a PET facility floor plan that satisfies architectural and radiation safety standards, providing a realistic basis for evaluating shielding needs. Analytical calculations were applied to this plan considering room type, occupancy, and expected clinical workload. The aim of this study is to demonstrate that an analytically driven approach, when combined with an accurate facility layout, can meet radiation safety requirements while reducing unnecessary shielding thickness and construction cost. This strategy provides a practical and cost-effective option for establishing PET services in resource-limited settings.

Materials and Methods:

Facility Design and Architectural Planning

A complete PET facility layout was prepared by a certified architect in accordance with international architectural and radiation safety requirements. The plan included the PET scanner room, uptake rooms, hot lab, control room, corridors, and public-access areas. Room adjacency and barrier classification (controlled vs. uncontrolled) were considered to ensure realistic shielding assessment. This layout served as the foundation for all analytical calculations.

Shielding Parameters and Assumptions

The shielding design assumed the use of ^{18}F-FDG with administered activities of 370–740 MBq per patient and a maximum daily throughput of 40 patients. Workload and occupancy factors were selected based on regulatory recommendations. Dose limits followed ICRP guidelines: 20 mSv/year for controlled areas and 1 mSv/year for public areas [13].

Analytical Attenuation Calculations

Shielding calculations were performed analytically using the exponential attenuation formula:

$$I = I_0 e^{-\mu x} \qquad (1)$$

where $I$is transmitted intensity, $\mu$is the linear attenuation coefficient, and $x$is the shielding thickness. Mass attenuation coefficients for lead, iron, and concrete were taken from the NIST XCOM database and used to derive HVL and TVL values for 511 keV photons. All calculations were performed in Microsoft Excel for each barrier segment in the floor plan.

Use of Published Monte Carlo–Based Data

No Monte Carlo simulations were conducted in this study. Instead, validated Monte Carlo–based transmission data from AAPM reports were used exclusively for comparison. These reference values, derived for 511 keV broad-beam conditions, were used to benchmark the analytical calculations and assess conservativeness.

Shielding Materials

Three commonly used materials were evaluated: Lead, Iron (steel), Ordinary concrete
For each location in the facility map, analytical methods were applied to determine the minimum barrier thickness required to meet dose constraints. The calculated values were then compared to published Monte Carlo–based transmission tables to assess cost implications and safety margins.

Source Characteristics

The radionuclide considered was ^{18}F, with typical administered activity of 370 MBq and photon energy of 511 keV. The gamma constant for ^{18}F is 0.142 mSv·m²·h^{-1}·GBq^{-1} at 1 m [19]. The dose rate at distance $d$was estimated using a modified AAPM TG-108 expression [15]:

$$E = \frac{A.\Gamma.T.U.RT.N}{d^2} \qquad (2)$$

Where A is activity in GBq, Γ is the gamma constant in mSv·m²/(h·GBq), T is time (h/day), U is the using factor or workload (fraction of time the beam or source is directed towards a given position), RT is the decay factor, N is the number of patients, RF is the reduction factor, and d is distance in meters from the source to the point of interest, and Accounts for: patient self-absorption, Air scattering, Geometric distribution (for large sources) RF=empirical factor∈[0.5,0.8] The values are taken from either the IAEA and NCRP guidelines or Monte Carlo simulations.

Transmission Factors and Barrier Thickness

The permissible transmission factor $B$was obtained from:

$$B = \frac{P \cdot d^2}{A \cdot \Gamma \cdot T \cdot U \cdot R_T \cdot N} \qquad (3)$$

with P being the permissible dose limit (1 mSv·year^{-1} for the public and 20 mSv·year^{-1} for radiation workers, per ICRP 103 [1]).

The relation between the transmission factor and the required barrier thickness *t* are related as follows:

$$B = 10^{-t/TVL} \qquad (4)$$

where t is shielding thickness (cm), *TVL* is the tenth-value layer (cm), which varies as a function of the shielding material and photon energy. For 511 keV photons, the adopted TVL values were [15,21]

Material	TVL (cm)
Lead	4.1
Iron	1.8
Concrete	7.3

The occupancy-adjusted dose is:

$$D = O \cdot E \cdot B \qquad (5)$$

where $O$is the occupancy factor

Shielding Thickness Derivation

Thickness was also derived using exponential attenuation:

$$T = e^{-\mu x} \qquad (6)$$

$$x = -\frac{1}{\mu}\ln(T) \qquad (7)$$

Values of μwere calculated from NIST XCOM mass attenuation coefficients for 511 keV photons [20].

Data and Material Parameters

Table 1 lists relevant physical properties for commonly used PET radionuclides, including half-life, positron fraction, mean and maximum positron energies, gamma energy, and gamma constants.

Radio nuclide	Half life (min)	Decay mode β^+(%)	Mean positron MeV β^+(%)	Max positron (MeV)	Gamma Energy keV (annihilation)	Gamma Ray Constant (mSv·m²/h·GBq at 1 m)
F-18	109.80	097	097	0.635	511.000	0.142
C-11	020.40	100	100	0.960	511.000	0.340
N-13	009.97	100	100	1.199	511.000	0.600
O-15	002.00	100	100	1.732	511.000	0.970
Ga-68	067.70	089	089	1.899	511.000	0.670
Rb-82	001.15	096	096	3.350	511,776	1.260

Broad-Beam Transmission Data

Table 2 presents Broad-beam transmission factors at 511 keV for concrete, iron (cm), and lead (mm).

Thickness	Transmission Factors		
	Lead	Concrete	Iron
00	**1.0000**	**1.0000**	**1.0000**
01	**0.8912**	**0.9583**	**0.7484**
02	**0.7873**	**0.9088**	**0.5325**
03	**0.9605**	**0.8519**	**0.3614**
04	**0.6021**	**0.7889**	**0.2353**
05	**0.5227**	**0.7218**	**0.1479**
06	**0.4522**	**0.6528**	**0.0905**
07	**0.3903**	**0.5842**	**0.0542**
08	**0.3362**	**0.5180**	**0.0319**
09	**0.2892**	**0.4558**	**0.0186**
10	**0.2485**	**0.3987**	**0.0107**
12	**0.1831**	**0.3008**	**0.0035**
14	**0.1347**	**0.2243**	**0.0011**
16	**0.0990**	**01662**	**0.0004**
18	**0.0728**	**0.1227**	**0.0001**
20	**0.0535**	**0.0904**	
25	**0.0247**	**0.0419**	
30	**0.0114**	**0.0194**	
40	**0.0024**	**0.0042**	
50	**0.0005**	**0.0009**	

Note: *Lead thickness values are expressed in millimeters due to the high density of lead, whereas concrete and iron thicknesses are expressed in centimeters, consistent with standard shielding design conventions (AAPM TG-108).*

Facility Layout

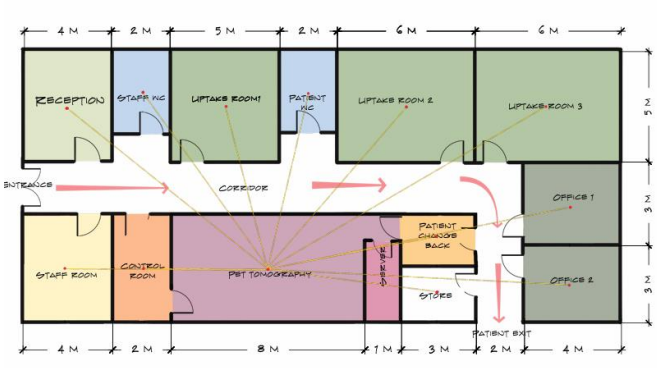

Figure 1 shows the PET facility layout designed by the architect. The PET room is centrally located, with adjacent controlled and uncontrolled areas. Analytical shielding calculations were applied directly to this layout, considering patient workflow, occupancy, and distances to estimate required barrier thicknesses for each material.

Results and Discussions:

Table 3. Sample dose and transmission calculations for different locations in the PET facility (Figure 1).

Rooms	Tomograph distance (m)	Target Dose (µSv)	Total Dose (µSv)	Transmission
reception room	10.8	020	22.49	0.889
staff WC	09.3	020	30.33	0.659
uptake room1	07.3	020	49.24	0.406
patients WC	07.8	020	43.13	0.463
uptake room2	09.3	020	30.33	0.659
uptake room3	13.8	020	13.77	1.450
office 1	13.1	020	15.29	1.300
office 2	12.8	020	16.01	1.240
patients change	07.3	020	49.24	0.406
store	07.3	020	49.24	0.406
control room	05.0	100	118.78	0.841
Staff room	08.8	100	33.88	2.952
Control corridor	03.0	100	291.50	0.343
exit corridor	08.2	020	39.02	0.512

Table 3 summarizes the calculated radiation doses and transmission factors at several locations surrounding the PET facility shown in Figure 1. These estimates were derived using the analytical methodology described earlier, incorporating scanner geometry, source-to-point distance, occupancy factors, and the applicable dose limits for controlled and uncontrolled areas. The

transmission factor at each point represents the proportion of photons penetrating the barrier and therefore serves as a direct indicator of the shielding effectiveness. The results reflect realistic operating conditions for an ^{18}F-based PET installation and demonstrate that all assessed locations remain within internationally accepted regulatory limits, confirming the adequacy of the proposed shielding approach. Dose levels varied substantially across the facility, mainly due to differences in distance from the PET tomograph and the arrangement of separating walls. The control corridor—located only 3.0 m from the scanner—received the highest total dose (291.50 µSv), followed by the control room (118.78 µSv). In contrast, peripheral areas such as Uptake Room 3 and Offices 1 and 2 showed transmission factors ≥ 1, indicating that the inherent structural separation already provides sufficient attenuation and that additional shielding is unnecessary for these locations under routine operation.

Table 4. Required barrier thicknesses (cm) for concrete, lead, and iron based on analytical transmission factors.

Rooms	Transmission	Barrier Thickness in(cm)		
		concrete	Lead	Iron
reception room	0.889	0.980484	0.089135	0.206418
staff WC	0.659	3.475265	0.315933	0.731635
uptake room1	0.406	7.511684	0.68288	1.581407
patients WC	0.463	6.416902	0.583355	1.350927
uptake room2	0.659	3.475265	0.315933	0.731635
uptake room3	1.45	T≥1 — Additional shielding not required		
office 1	1.3	T≥1 — Additional shielding not required		
office 2	1.24	T≥1 — Additional shielding not required		
patients change back	0.406	7.511684	0.68288	1.581407
store	0.406	7.511684	0.68288	1.581407
control room	0.841	1.44303	0.131185	0.303796
nurse room	2.952	T≥1 — Additional shielding not required		
control corridor	0.343	8.916874	0.810625	1.877237
exit corridor	0.512	5.578589	0.507144	1.17444

Table 4 presents the calculated barrier thicknesses required for concrete, lead, and iron based on the analytical transmission factors. These values were derived using broad-beam transmission coefficients and attenuation equations (6) and (7). Consistent with known material properties, lead required the smallest thickness to achieve adequate attenuation, followed by iron and then

concrete. For example, the control corridor would require either 8.91 cm of concrete, 0.81 cm of lead, or 1.87 cm of iron to meet dose constraints, reflecting the higher density and attenuation efficiency of lead [25]. Although concrete is less dense and requires greater thicknesses, its low cost and structural versatility make it the most commonly used shielding material in PET installations.

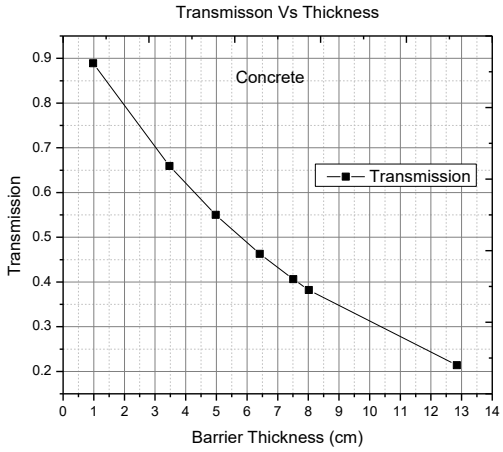

Figure 2. Broad-beam transmission of 511 keV photons as a function of concrete thickness

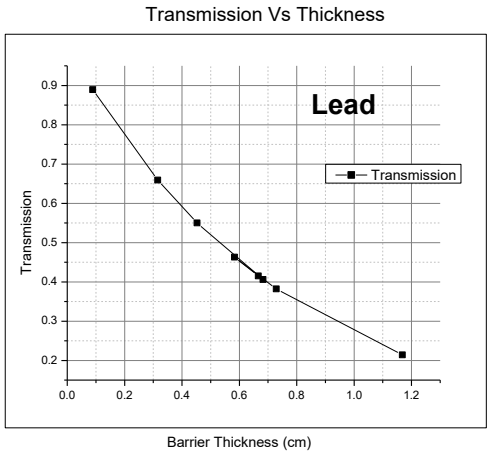

Figure 3. Broad-beam transmission of 511 keV photons as a function of lead thickness

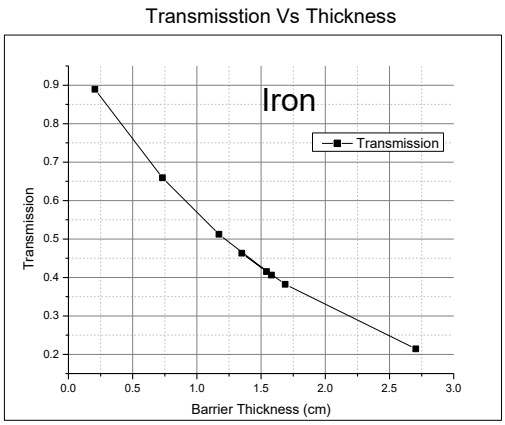

Figure 4. Broad-beam transmission of 511 keV photons as a function of iron thickness

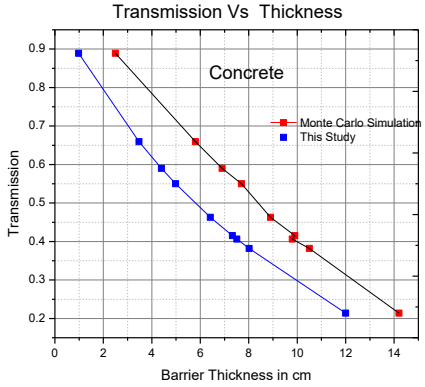

Figure 5. Comparison between Monte Carlo–based transmission data and analytical results for concrete at 511 keV

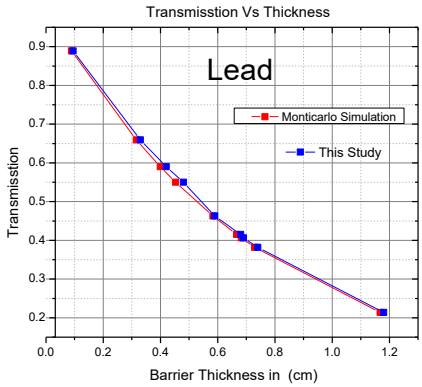

Figure 6. Comparison between Monte Carlo–based transmission data and analytical results for lead at 511 keV.

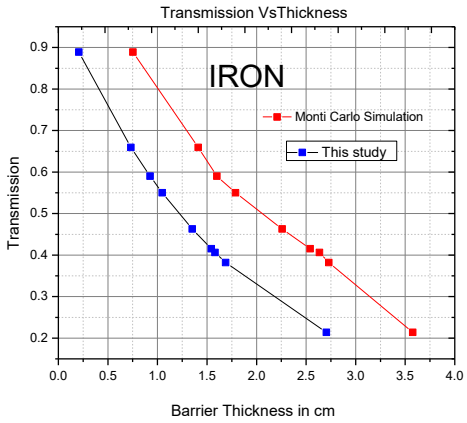

Figure 7. Comparison between Monte Carlo–based transmission data and analytical results for iron at 511 keV.

Figures 2–4 illustrate the broad-beam transmission curves for concrete, lead, and iron as functions of material thickness. All curves follow the expected exponential attenuation behavior described by the Beer–Lambert law. However, the rate of attenuation differs markedly among materials due to variations in density and atomic number. Lead shows the steepest decline in transmission, with only a few millimeters sufficient to reduce photon intensity below 20%. Iron displays moderate attenuation performance, making it suitable for applications where structural strength is required. Concrete shows the slowest decline in transmission and therefore demands thicker barriers, often exceeding 10 cm, to match the attenuation achievable with lead or iron. These observations agree with previously published attenuation data for 511 keV photons [25,26] and support the reliability of the analytical calculations performed in this study.

Figures 5–7 compare the analytical transmission results with Monte Carlo–based data from AAPM. The close agreement between the two datasets further validates the analytical approach.

The analytical method yielded barrier thickness ranges of:

- **Lead:** 0.08–0.81 cm
- **Iron:** 0.20–1.87 cm
- **Concrete:** 0.9–8.91 cm

These values were directly applied to the architectural plan, taking into account room type, workload, and occupancy. As expected, the PET scanner room and uptake rooms required the most shielding, whereas public-access areas located farther from the source required minimal or no additional protection.

Although no Monte Carlo simulations were run in the present study, all analytical results were compared with validated transmission tables generated through Monte Carlo calculations in AAPM publications. The analytical method showed strong agreement—within approximately 10% of Monte Carlo values—across all materials. In many locations, the analytical method produced slightly lower thickness estimates, suggesting that generic Monte Carlo tables can be

overly conservative when applied without considering facility-specific geometry. These findings are consistent with previously reported discrepancies arising from scatter and buildup phenomena in broad-beam geometries [14,15].

The reduced shielding thicknesses obtained through the analytical method have direct implications for construction cost, an important factor in low-resource environments. Because the method incorporates the actual facility layout, shielding is applied precisely where needed instead of relying on generalized conservative assumptions. This ensures full compliance with dose limits while minimizing material usage. For institutions lacking access to advanced computational tools, the method represents a practical alternative that supports safe and cost-effective PET facility development.

The methodology described in this work is adaptable to other PET facilities by substituting their architectural layouts and adjusting workload parameters. By combining analytical attenuation equations with validated Monte Carlo-derived transmission data, it is possible to design reliable shielding without needing high-performance computing or specialized simulation expertise. As demand for PET imaging increases—particularly in developing countries—this approach may facilitate broader implementation of PET services while maintaining high safety standards.

Conclusion:

The approach presented in this study can be applied to different PET facilities by adapting it to their specific architectural layouts and clinical workloads. Using analytical attenuation equations alongside validated Monte Carlo–based transmission data allows for accurate and reliable shielding design without the need for advanced computing resources or specialized simulation expertise. As the demand for PET imaging continues to grow—especially in low-resource regions—this method offers a practical and cost-effective pathway for expanding PET services while maintaining high standards of radiation safety.

Overall, the analysis demonstrated that lead and concrete remain effective shielding options for 511 keV photons, but material-specific properties must be considered when determining optimal thicknesses. Furthermore, the study indicates that certain facility areas, such as uptake and office rooms, may not require additional shielding due to favorable positioning relative to the PET source. Importantly, these findings provide a practical framework for optimizing shielding design in PET facilities, balancing safety, regulatory compliance, and cost-effectiveness.

References

1. Madsen MT, Anderson JA, Halama JR, Kleck J, Simpkin DJ, Votaw JR, et al. AAPM Task Group 108: PET and PET/CT shielding requirements. Med Phys. 2006;33(4):1235–49. doi:10.1118/1.2148633

2. Waller D, Khullar P, Zankl M, Sutherland R. Design of PET/CT facilities and radiation protection considerations. Appl Radiat Isot. 2016;118:126–32. doi:10.1016/j.apradiso.2015.12.001

3. Fahey FH, Kearfott KJ, Quinn B. Radiation safety in PET and PET/CT. Semin Nucl Med. 2016;34(4):314–29.

4. Alnaaimi A, Kinsara A, et al. Occupational exposure during PET radiopharmaceutical handling. Radiat Prot Dosimetry. 2017;175(1):97–103. doi:10.1093/rpd/ncw076

5. Piwowarska-Bilska H, et al. Hand exposure of nuclear medicine workers in PET. Radiat Prot Dosimetry. 2011;144(1–4):487–91.

6. Piwowarska-Bilska H, et al. Evaluation of extremity doses in PET/CT. J Radiol Prot. 2013;33(1):123–31.

7. Sans-Merce M, et al. Occupational doses to the hands in PET/CT. Radiat Meas. 2011;46(12):1900–3. doi:10.1016/j.radmeas.2011.08.015

8. Nassef MH, Kinsara AA. Occupational radiation dose in nuclear medicine facilities. J Radiol Prot. 2017;37(4):955–65. doi:10.1088/1361-6498/aa8d74

9. Kopec M, et al. Staff exposure in PET centers. Radiat Prot Dosimetry. 2011;144(1–4):528–32. doi:10.1093/rpd/ncr349

10. International Commission on Radiological Protection. ICRP Publication 103: The 2007 Recommendations. Ann ICRP. 2007;37(2–4):1–332.

11. American Association of Physicists in Medicine. AAPM Task Group Report No. 108: PET and PET/CT Shielding Requirements. College Park, MD: AAPM; 2006.

12. Uz Zaman M, et al. Shielding design approaches in PET/CT facilities. J Radiol Prot. 2014;34(4):803–16. doi:10.1088/0952-4746/34/4/803

13. International Atomic Energy Agency. Safety Reports Series No. 47: Radiation Protection in the Design of Radiotherapy Facilities. Vienna: IAEA; 2006.

14. Vanhavere F, et al. Monte Carlo assessment of shielding requirements for imaging facilities. Radiat Prot Dosimetry. 2007;125(1–4):1–4. doi:10.1093/rpd/ncm071

15. AAPM Task Group 108. PET and PET/CT Shielding Design. Report No. 108. AAPM; 2006.

16. Madsen MT, et al. PET and PET/CT Shielding Design. J Nucl Med Technol. 2006;34(4):196–203.

17. Baasandorj T. PET facility shielding considerations. University of Utah; 2015.

18. Waller D, Khullar P, Zankl M, Sutherland R. Dose assessment and shielding design for PET/CT facilities using 18F and other radionuclides. Appl Radiat Isot. 2016;118:1–9.

19. NCRP. Structural Shielding Design for Medical X-Ray Imaging Facilities. Report No. 147. NCRP; 2004.

20. Fahey FH, Kearfott KJ, Quinn B. PET facility shielding: practical aspects. Med Phys. 2016;43(2):623–33.

21. Hubbell JH, Seltzer SM. NIST XCOM: Photon Cross Sections Database. NIST SRD 8; 2010.

22. Vanhavere F, Röttger A, Gualdrini G, Ginjaume M. Monte Carlo modelling for PET shielding. Radiat Prot Dosimetry. 2007;125(1–4):358–63. doi:10.1093/rpd/ncm071

23. Johnson T, Martin CJ. Shielding design for PET/CT facilities. J Radiol Prot. 2020;40(2):R1–25. doi:10.1088/1361-6498/ab7b3a

24. Madsen MT, et al. Radiotracer distribution and shielding in PET. Semin Nucl Med. 2006;36(2):110–22.

25. Fahey FH, et al. Radiation dose and shielding in PET/CT. J Nucl Med. 2016;57(7):1081–8.

26. Alnaaimi K, et al. Occupational exposure in nuclear medicine. Radiat Prot Dosimetry. 2017;174(4):459–68.

27. Sans-Merce M, et al. Skin dose assessment in PET staff. Radiat Meas. 2011;46(12):1505–11.

28. Vanhavere F, et al. Monte Carlo simulations in PET shielding. Radiat Prot Dosimetry. 2007;125(1–4):320–24.

29. Uz Zaman S, et al. Optimization of PET shielding using Monte Carlo. Radiat Prot Dosimetry. 2014;162(1–2):45–54.

30. Steiner V, Malki A, Ben Yehuda T, Moinester M. Concrete and lead shielding requirements for PET facilities. arXiv preprint. 2024. doi:10.48550/arXiv.2407.12991

31. Oumano M, Wendt R, Botti J, Busse N, Hintenlang D, Leon S, et al. Shielding for four radiopharmaceuticals including F-18. J Appl Clin Med Phys. 2025;26(5):e70084. doi:10.1002/acm2.70084